Journal of Achievements in Materials and Manufacturing Engineering
VOLUME 36
ISSUE 1
September
2009

Effect of the sintering parameters on structure of the gradient tool materials

L.A. Dobrzański*, J. Hajduczek, A. Kloc-Ptaszna
Division of Materials Processing Technology, Management and Computer Techniques in Materials Science, Institute of Engineering Materials and Biomaterials, Silesian University of Technology, ul. Konarskiego 18a, 44-100 Gliwice, Poland
* Corresponding author: E-mail address: leszek.dobrzanski@polsl.pl

Received 20.04.2009; published in revised form 01.09.2009

Properties

ABSTRACT

Purpose: The purpose of this work was to obtain gradient tool materials, based on the unalloyed steel reinforced with HS6-5-2 high-speed steel, through using the conventional powder metallurgy method and sintering in the vacuum furnace at the range of temperature from 1190°C to 1250°C, in steps of 20°C, for 30 and 60 minutes.

Design/methodology/approach: In presented work gradient materials were obtained through powder metallurgy consisting uniaxial compacting method and sintering. The unalloyed steel was fabricated by mixing iron and graphite powders. Structural examinations were carried out by optical microscopy methods assisted with the computer image analysis, scanning electron microscopy and X-ray microanalysis.

Findings: It was found out, that increase of the sintering temperature contribute to the undergo coagulation on the grain boundary or creation of the large allocations on the grain boundary of the carbides in the matrix. As well, it was proved, that incompleted sintering process was caused by too low sintering temperature.

Practical implications: Such gradient material may be applied for turning tools.

Originality/value: A forming methods were developed for unalloyed steel and high-speed steel powders, which made it possible to obtain specimens with six layers in its structure. The material presented in this paper has layers, at one side consisting unalloyed steel and at the other side high-speed steel. The layers inside the material are mixes of the high-speed steel and unalloyed steel powders in the relevant proportions.

Keywords: Powder metallurgy; FGM; Tool materials; SEM

Reference to this paper should be given in the following way:
L.A. Dobrzański, J. Hajduczek, A. Kloc-Ptaszna, Effect of the sintering parameters on structure of the gradient tool materials, Journal of Achievements in Materials and Manufacturing Engineering 36/1 (2009) 33-40.

1. Introduction

Composites materials consisting of two different materials with a gradient changing of composition and structure over volume, which results in corresponding changes in its properties, are called Functionally Graded Materials (FGMs) [1-6].

There are various technologies that enable manufacturing of such materials like powder metallurgy methods or laser aided and plasma discharge methods [6-9]. Obtained material should provide high wear resistance of the outside layer, gradient composition in the intermediate layers and ability to carry high dynamic loads in the core layer. Material made by powder metallurgy methods offers extremely high wear resistance, that combines relatively high ductility of the core material and lower production costs, which is important feature in materials designed for turning tools, hot-working plastic forming tools and tools used for high-speed operations [4-8,10,11].

The main objective of this work is to investigate influence of the sintering parameters on the structure of the designed material.

2. Material and experimental procedure

The investigations were made using the test pieces made of the high-speed steel H-S6-5-2 and unalloyed steel containing 1.7% carbon. Unalloyed steel was obtained from the mixture of graphite and iron powders, and high-speed steel was obtained from water-atomized powder. The iron powder were produced by ECKA Granules Poudmet S.A.S. (France) and grain size was <50 µm. JLQ ISMAF S.L. (Spain) produced natural graphite powders; for 99.5% grain size was <40 µm, and for 50% grain size was <18 µm. Producer of the HS6-5-2 high-speed steel powder was Höganäs AB (Sweden). The powder grain size was >150 µm. The chemical composition of the used high-speed steel powders is presented in Table 1.

Table 1.
Chemical composition of HS6-5-2 high-speed steel powder

Chemical element	Mass concentration, %
C	0.75-0.9
Mn	0.2-0.45
Cr	3.75-4.5
W	5.5-6.75
Mo	4.5-5.5
V	1.6-2.2
Si	≤0.45
P and S	≤0.04
Ni	≤0.2
Co and Cu	≤0.1

The uniaxial compacting method was used for making the prepregs. The specimens had six layers: from the unalloyed steel at the bottom, through four intermediate layers containing 80 to 20% unalloyed steel (participation of unalloyed steel and high-speed steel change by 20%), to upper layer which was made from 100% high-speed steel powder. Compacting was carried out in the uniaxial unilateral die (Fig. 1), under 500 MPa pressure. Next, the test pieces were sintered in the vacuum furnace at the temperature of 1190°C, 1210°C, 1230°C and 1250°C for 30 and 60 minutes. The cooling rate was 5°C/min.

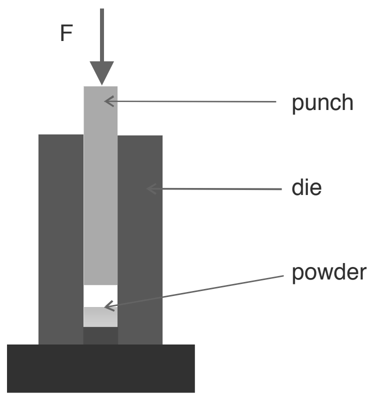

Fig. 1. Scheme of the uniaxial unilateral die

Before the porosity research, samples were mechanically grinded and polished. Investigations were carried out on a optical microscope Axiowert 405M assisted with the computer image analysis program Image-ProPlus. The porosity of the material was measured for layers containing 100% high-speed steel HS6-5-2 and 100% unalloyed steel. Measurements were carried out in ten random areas of both investigated layers. Results obtained from porosity measurements were elaborated statistically.

Next, specimens were etched in nital (3% HNO_3 in C_2H_5OH), than observed on a optical microscope (20-1000x mag.) and scanning electron microscopes SEM XL30 (Philips Co.) and SUPRA 25 (Zeiss) equipped with the back-scattered electrons detector (BSE) and the dispersive energy analyser (EDAX D4). The range of accelerating voltage of used scanning electron microscopes' was from 15 to 20 kV and their magnification was from 40x to 10000x.

3. Results and discussion

A SEM BSE micrograph of the sintered test pieces in the cross-section are shown in Figure 2. The six layer structure of the gradient material sintered at 1230ºC for 60 min appeared to be less porous than the same material sintered at 1190ºC for 30 min. Its structure is more uniform and the particular layers cannot be seen so easily as in the specimen sintered in lower temperature.

a)

b)

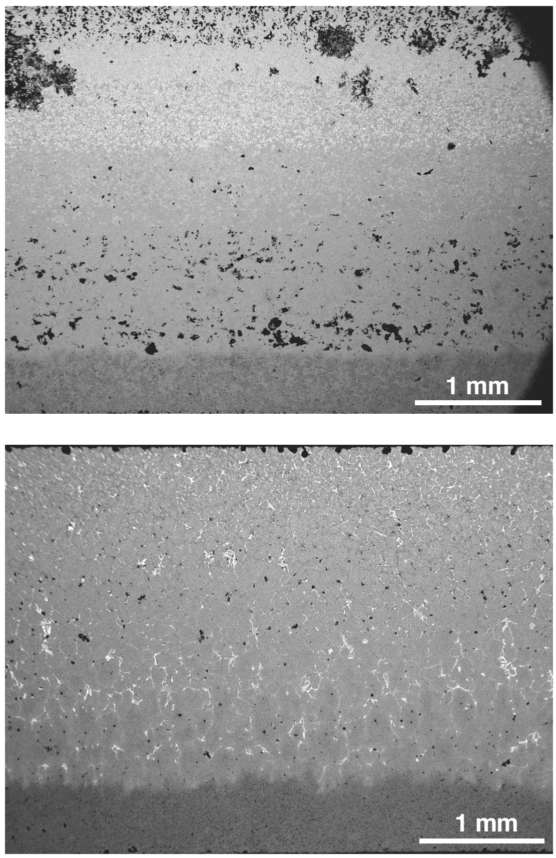

Fig. 2. SEM (BSE) micrograph of the specimens' cross-section; sintering temperature and time: a) 1190ºC for 30 min, b) 1230ºC for 60 min; (upper layer: 100% high-speed steel HS6-5-2, bottom layer: 100% unalloyed steel C170); etched in nital

Structure of the individual layers of specimens sintered at the temperatures of 1190ºC, 1210ºC, 1230ºC and 1250ºC for 60 and 30 min respectively are shown at Figures 3-12 and Figures 15, 16.

The microstructure of the outer layer containing 100% high-speed steel HS6-5-2, sintered at 1230ºC for 60 min, is partly melted, what is typical for such kind of steel (Fig. 3). Some of the carbides have a shape characteristic for eutectic carbides, which indicate crystallisation from liquid between austenite grains. Carbides located on the grains boundaries are large and partly coagulated, whereas small carbides are observed inside grains. Similar microstructure occurred in a layer containing 80% high-speed steel HS6-5-2, and 20% unalloyed steel C170 (Fig. 4).

a)

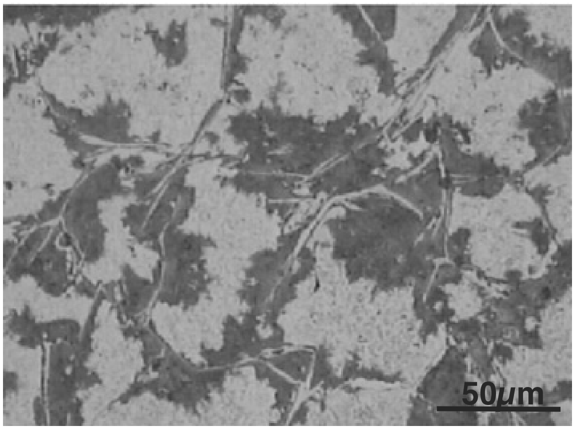

b)

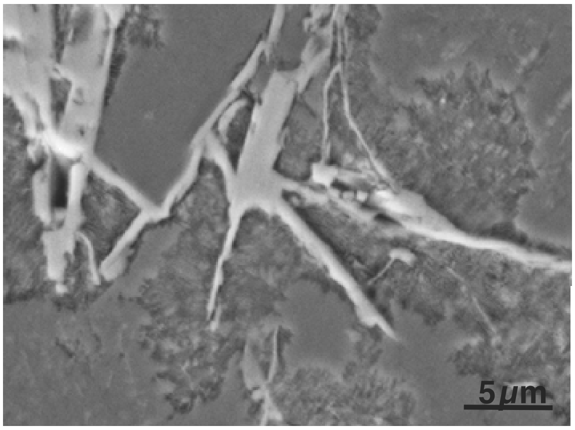

Fig. 3. Structure of the specimen, layer containing 100% high-speed steel HS6-5-2, sintered at the temperature of 1230ºC for 60 min; a) optical microscope, b) SEM (BSE); etched in nital

Observation of the specimens sintered at 1210ºC show that carbides are in the initial stage of coagulation (Fig. 5)

Carbides observed in the intermediate layers are elongated and placed on the grain boundaries (Figs. 6, 7). Decreasing mass fraction of the high-speed steel HS6-5-2 results in the increasing of porosity (dark areas in Figure 8).

a)

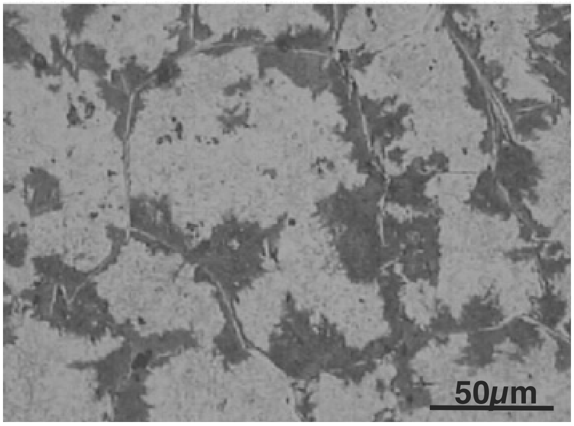

b)

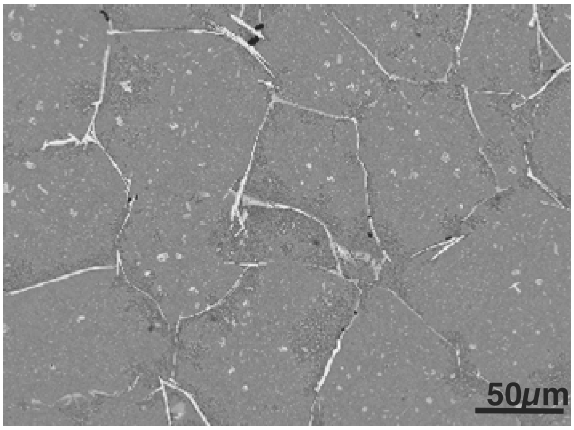

Fig. 4. Structure of the specimen, layer containing 80% high-speed steel HS6-5-2 and 20% unalloyed steel, sintered at the temperature of 1230ºC for 60 min; a) optical microscope, b) SEM (BSE); etched in nital

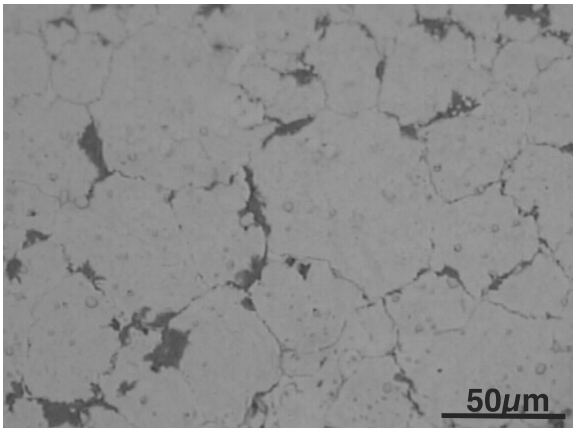

Fig. 5. Structure of the specimen, layer containing 100% high-speed steel HS6-5-2, sintered at the temperature of 1210ºC for 30 min; optical microscope; etched in nital

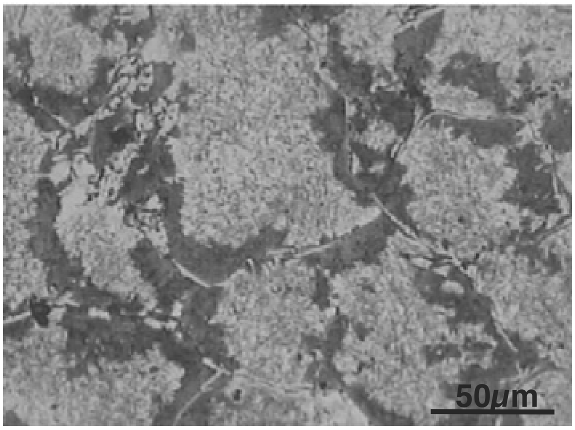

Fig. 6. Structure of the specimen, layer containing 60% high-speed steel HS6-5-2 and 40% unalloyed steel, sintered at the temperature of 1230ºC for 60 min; optical microscope; etched in nital

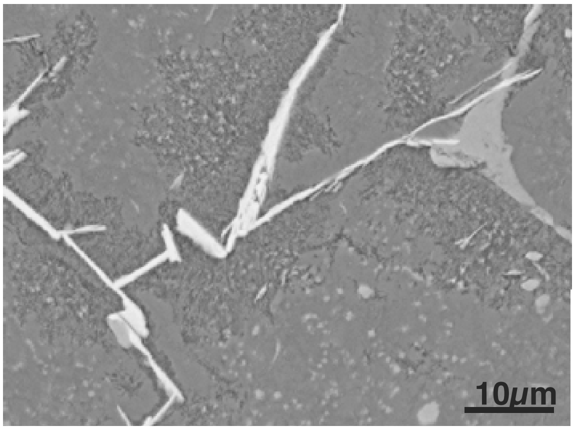

Fig. 7. Structure of the specimen, layer containing 40% high-speed steel HS6-5-2 and 60% unalloyed steel, sintered at the temperature of 1230ºC for 60 min; SEM (BSE); etched in nital

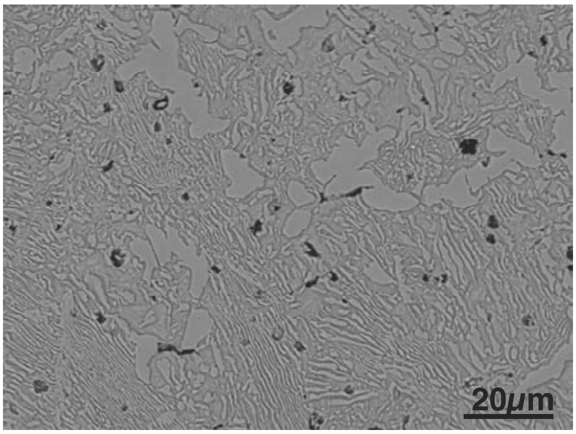

Fig. 8. Structure of the specimen, layer containing 100% unalloyed steel, sintered at the temperature of 1190ºC for 60 min; SEM (BSE); etched in nital

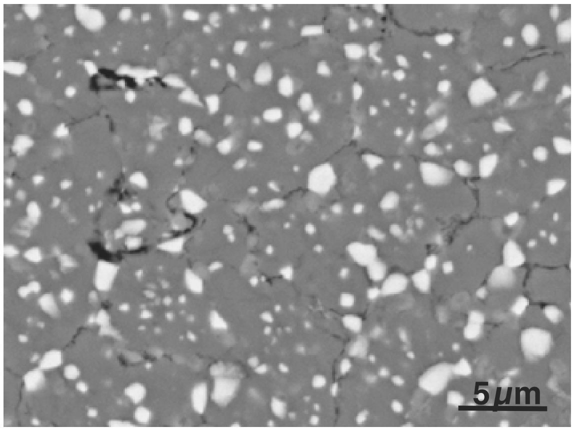

Fig. 9. Structure of the specimen, layer containing 80% high-speed steel HS6-5-2 and 20% unalloyed steel, sintered at the temperature of 1190ºC for 30 min; SEM (BSE); etched in nital

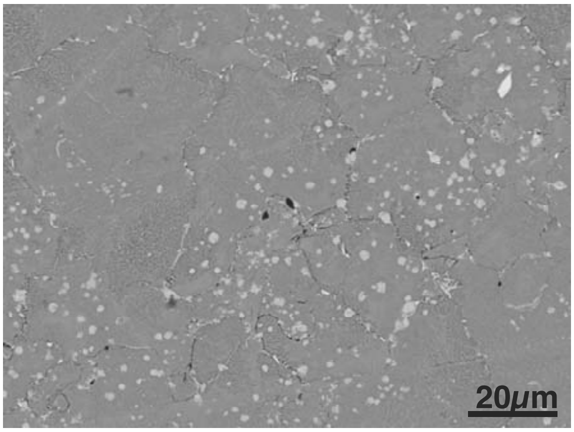

Fig. 10. Structure of the specimen, layer containing 40% high-speed steel HS6-5-2 and 60% unalloyed steel, sintered at the temperature of 1190ºC for 30 min; SEM (BSE); etched in nital

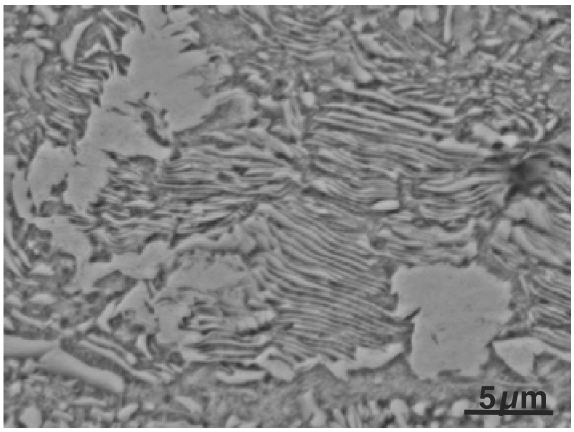

Fig. 11. Structure of the specimen, layer containing 100% unalloyed steel, sintered at the temperature of 1230ºC for 60 min; SEM (BSE); etched in nital

Discontinuity of the grains boundaries observed in the intermediate layers of the specimens, sintered at temperature 1190ºC, are prove of incompleted sintering process (Figs. 9, 10).

Investigated inner layers containing 100% unalloyed steel appeared microstructure of pearlite surrounded by irregular grains of the pro-eutectoid cementite (Figs. 8, 11, 12). Pearlite observed in this layer is thicker than in next layer, which contains 20% high-speed steel HS6-5-2.

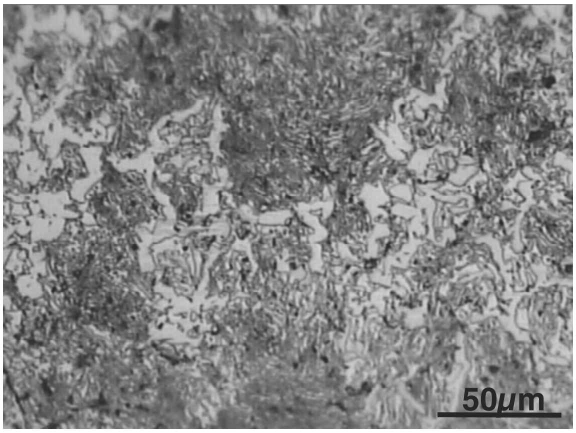

Fig. 12. Structure of the specimen, boundary between layer containing 100% unalloyed steel and layer containing 20% high-speed steel HS6-5-2 and 80% unalloyed steel, sintered at the temperature of 1210ºC for 30 min; optical microscope; etched in nital

It was found out, based on the porosity measurements carried out for specimens sintered at 1190, 1210 and 1230°C for 30 minutes, that layers containing 100% high-speed steel HS6-5-2 show repeatedly lesser porosity than layers containing 100% unalloyed steel (Fig. 13, Table 2).

Specimen sintered at 1190°C for 30 min reveal maximum porosity difference, about 11%, between inner and outer layers. Average value of the porosity, in the layers containing 100% high-speed steel HS6-5-2, incorporate range from 0.7 to 0.9%. Whereas, increasing of the sintering temperature has significant effect on lowering of the porosity of the layers containing 100% unalloyed steel (Table 2).

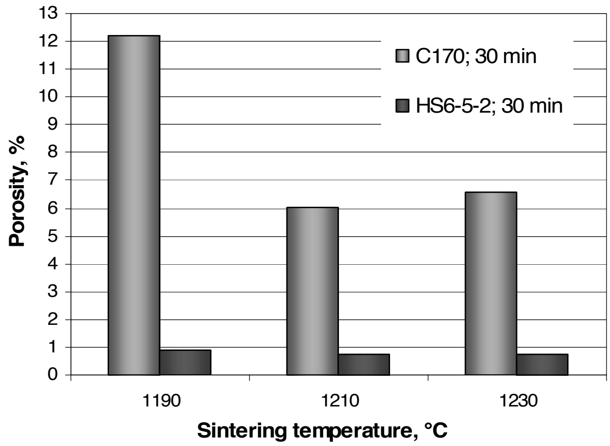

Fig. 13. Effect of the sintering temperature on the porosity of the layers containing 100% unalloyed steel and 100% high-speed steel HS6-5-2; sintering time: 30 minutes

As well, it was found out that layers containing 100% high-speed steel HS6-5-2 sintered at the temperatures of 1190, 1210 and 1230°C for 60 minutes, show repeatedly lesser porosity than layers containing 100% unalloyed steel (Fig. 14, Table 2).

Specimen sintered at 1190°C for 60 min reveal maximum porosity difference, about 7.7%, between inner and outer layers. The minimum porosity difference, about 1%, is shown in investigated layers sintered at the temperature of 1230°C for 60 minutes. The layers containing 100% high-speed steel HS6-5-2, sintered at 1190, 1210 and 1230°C for 60 minutes, show similar porosity (about 1%). Increase of the sintering temperature has significant effect on lowering of the porosity of the layers containing 100% unalloyed steel (Table 2).

Table 2.
Porosity measurements results

Material	Sintering parameters, °C/min	Results of the measurements and calculations, %			
		arithmetic mean	standard deviation	semi-interval of confidence	confidence interval for the arithmetic mean
HS6-5-2	1190/30	0.90	0.46	0.28	0.62-1.19
	1210/30	0.74	0.42	0.26	0.48-1.00
	1230/30	0.74	0.32	0.20	0.54-0.93
	1190/60	1.04	0.28	0.17	0.87-1.22
	1210/60	0.97	0.41	0.25	0.72-1.22
	1230/60	1.35	0.42	0.26	1.09-1.61
C170	1190/30	12.23	2.43	1.51	10.72-13.73
	1210/30	6.03	1.76	1.09	4.94-7.12
	1230/30	6.59	1.33	0.82	5.77-7.41
	1190/60	8.83	2.90	1.79	7.04-10.63
	1210/60	4.86	1.22	0.76	4.10-5.61
	1230/60	2.43	1.32	0.82	1.61-3.24

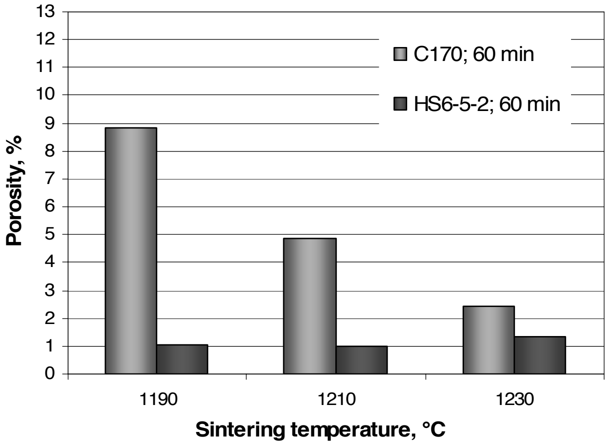

Fig. 14. Effect of the sintering temperature on the porosity of the layers containing 100% unalloyed steel and 100% high-speed steel HS6-5-2; sintering time: 60 minutes

Wide range of obtained confidence interval for the arithmetic mean testify for large dispersion of obtained results of the porosity measurements. It causing that layers containing 100% high-speed steel HS6-5-2 and sintered at 1190, 1210 and 1230°C do not reveal substantial absolute difference of the porosity. Layers containing 100% unalloyed steel show considerably bigger mean value of the porosity and by the reason of that, sintering parameters, which are most favourable for structure of the inner layer, should be decisive in case of selection of the sintering parameters for these particular gradient tool materials.

To obtain the lowest porosity of the unalloyed steel layers they have to be sintered at the temperature of 1230°C for 60 min. The test pieces, sintered at these conditions, are characterized by the lowest, about 1%, difference of the porosity between the extreme layers. Statistically elaborated results obtained from porosity measurements are listed in Table 2.

The EDX microanalysis were carried out for layers containing 100% high-speed steel HS6-5-2, and 20% high-speed steel HS6-5-2 and 80% unalloyed steel. Test pieces were sintered at temperature of 1250 ºC. Investigation of only metallic elements was caused by too low intensity of characteristic X-radiation of carbon, which had influence on results accuracy.

a) b) c)

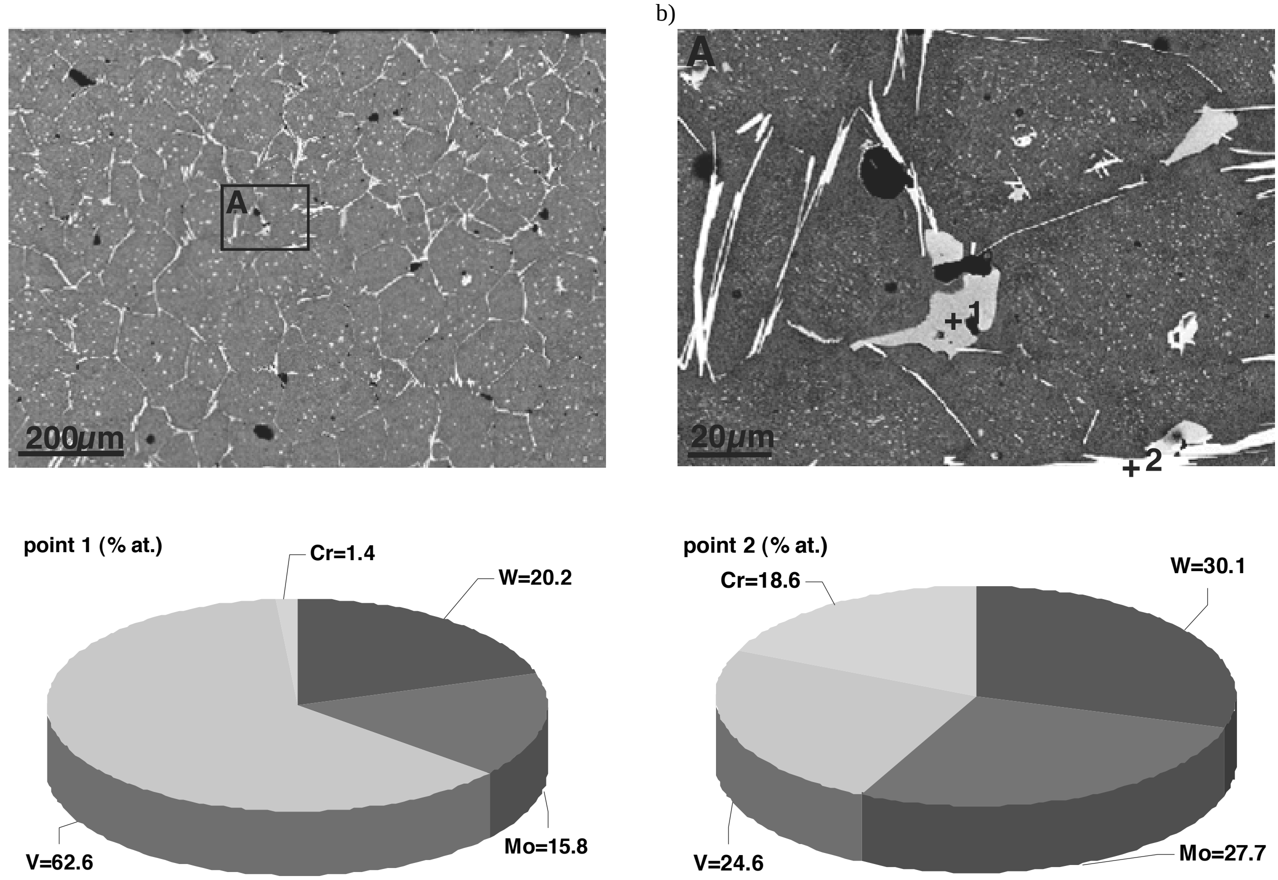

Fig. 15. Microstructure of the specimen, layer containing 100% high-speed steel HS6-5-2, sintered at the temperature of 1250ºC a) upper part of the test piece, b) range of the 100% high-speed steel HS6-5-2 (approximately 0.4 mm from specimen surface); a) and b) SEM BSE; c) diagrams with results of the EDX chemical composition microanalysis (without C) made in points marked in Fig. b)

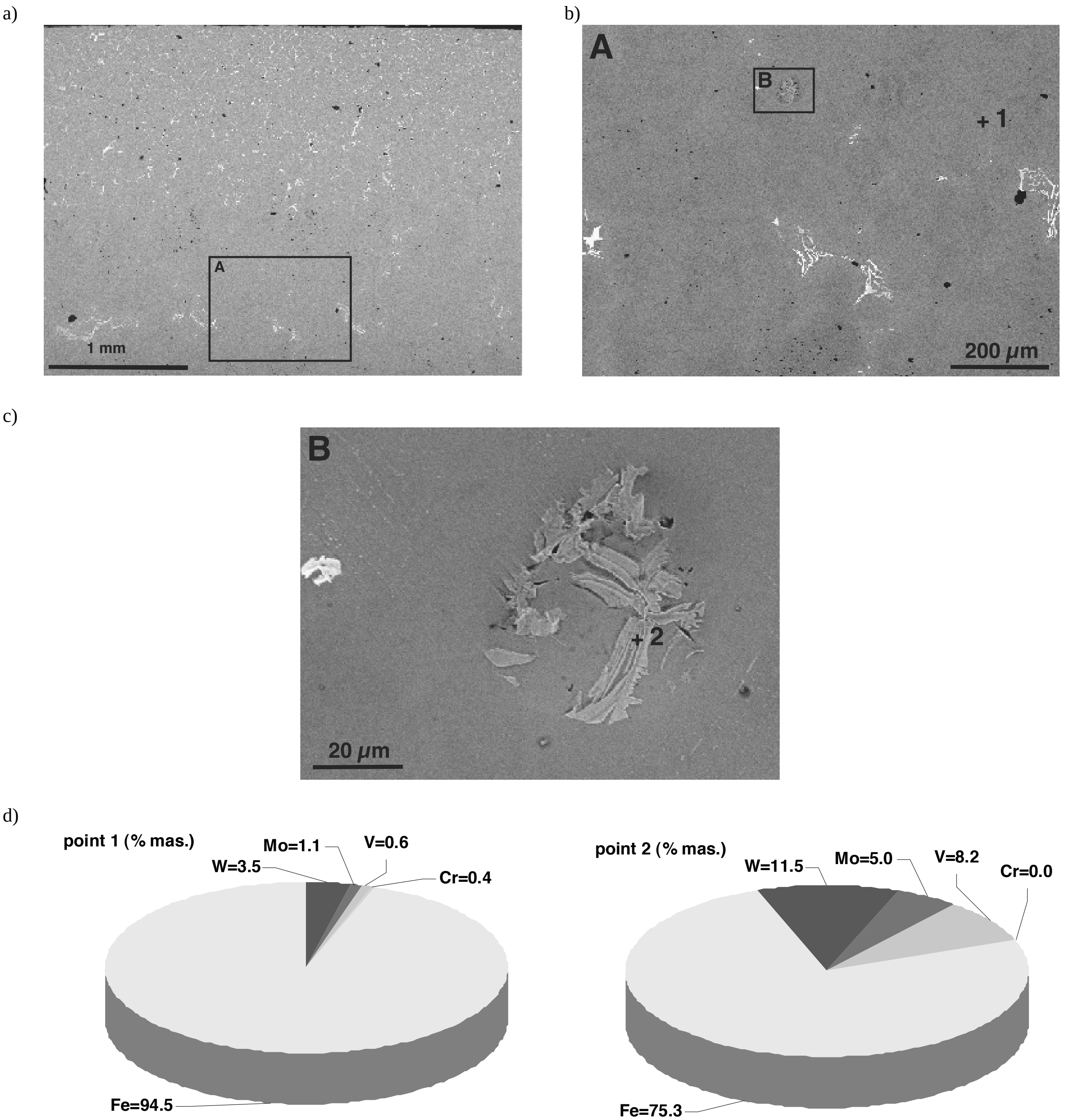

Fig. 16. Microstructure of the specimen, layer containing 20% high-speed steel HS6-5-2 and 80% unalloyed steel, sintered at the temperature of 1250ºC a) upper part of the test piece, b) and c) range of the 20% high-speed steel HS6-5-2 and 80% unalloyed steel (approximately 2.1 mm from specimen surface); a) - c) SEM BSE; d) diagrams with results of the EDX chemical composition micro-analysis (without C) made in points marked in Figs. b) and c)

Microstructure observations reveal significant differences in chemical composition of the middle of the grains and theirs boundaries (Figs. 15, 16). Results of the EDX microanalysis reveal higher concentration of carbide-forming elements, like W, Mo, V and Cr (Fig. 15), on the grain boundaries. In the Figure 15 those precipitations are brighter than the rest of the structure. Presumably, according to the references [12-15], white, rich in vanadium precipitations corresponds to MC type of carbides, whereas grey ones, rich in tungsten and molybdenum, represents the M_6C type of carbides. Except large carbides at the grains boundaries, small precipitations distributed inside grains were observed in the structure of layers containing high HS6-5-2 high-speed steel mass fraction (Figs. 15a, 16a).

Some of the small carbides, that occurs in the layer containing 20% high-speed steel HS6-5-2 and 80% unalloyed steel, have chemical composition mainly composed of iron with limited concentration of carbide-forming elements which suggest [4,6] that they might represents alloy cementite (M_3C type of carbides) (Fig. 16c, point 2). Decreasing concentration of carbide-forming elements in matrix material is caused by increasing distance from layer that contains 100% high-speed steel HS6-5-2 (Fig. 16).

4. Conclusions

It was found out, based on a investigations of the gradient materials with the unalloyed steel matrix, that increase of sintering temperature from 1190ºC to 1250ºC has greater effect on grains growth and carbides morphology than increase of sintering temperature from 30 to 60 minutes.

Due to the sintering parameters carbides are evenly distributed in the matrix or undergo coagulated on the grain boundary or create large allocations on the grain boundary. The temperature of 1190ºC is too low for sintering the HS6-5-2+C170 gradient material, as in the middle layers of the test piece, sintering process is not finished. The temperatures of 1250°C and 1230°C are too high, because during the sintering, partly melted structures, typical for high-speed steels, are made.

Layers containing 100% unalloyed steel appeared micro-structure of pearlite surrounded by irregular grains of the pro-eutectoid cementite.

Specimen sintered at 1190°C for 30 min reveal lowest porosity in the layers containing 100% high-speed steel HS6-5-2, while, sintering at the temperature of 1230°C for 60 minutes results in the lowest porosity of the layer containing 100% unalloyed steel. It was found out that sintering parameters, which are most favourable for structure containing 100% unalloyed steel layer, should be applied to manufacture these particular gradient materials.

Basing on the optical and scanning microscopy investigations, as well as, on the porosity measurements, it was found out that six-layer gradient material, based on the unalloyed steel reinforced with HS6-5-2 high-speed steel, presents the optimal structure, in all layers, after sintering in the temperature of 1210°C for 60 minutes.

References

[1] Y. Miyamoto, W.A. Kaysser, B.H. Rabin, A. Kawasaki, R.G. Ford, Functionally Graded Materials: Design, Processing and Applications, Kluwer Academic Publishers, Boston-Dordrecht-London, 1999.

[2] K. Ichikawa, Functionally Graded Materials in the 21st Century: A Workshop on Trends and Forecasts, Kluwer Academic Publishers, Boston, 2001.

[3] W. Lengauer, K. Dreyer, Functionally Graded Hardmetals, Journal of Alloys and Compounds 338 (2002) 194-212.

[4] J. Wessel, The Handbook of Advanced Materials: Enabling New Designs, Materials Technology Series, 2004.

[5] M.B. Bever, P.F. Duwez, Gradients in composite materials, Materials Science and Engineering 10 (1972) 1-8.

[6] J. Hajduczek, Effect of the sintering parameters on structure and properties of the gradient tool materials with the unalloyed steel matrix, MSc thesis, Silesian University of Technology, Gliwice, 2007 (in Polish).

[7] S. Suresh, A. Mortensen, Fundamentals of functionally graded materials, JOM Communications Limited, London, 1999.

[8] E.M. Ruiz-Navas, R. García, E. Gordo, F.J. Velasco, Development and characterisation of high-speed steel matrix composites gradient materials, Journal of Materials Processing Technology 143-144 (2003) 769-775.

[9] B. Kieback, A. Neubrand, H. Riedel, Processing techniques for functionally graded materials, Materials Science and Engineering 362 (2003) 81-106.

[10] L.A. Dobrzański, A. Kloc, G. Matula, J. Domagała, J.M. Torralba, Effect of carbon concentration on structure and properties of the gradient tool materials, Journal of Achievements in Materials and Manufacturing Engineering 17 (2006) 45-48.

[11] E.C. Lee, C.Y. Nian, Y.S. Tarng, Design of a dynamic vibration absorber against vibrations in turning operations, Journal of Materials Processing Technology 108 (2001) 278-285.

[12] L.A. Dobrzański, Effects of chemical composition and processing conditions on the structure and properties of high-speed steels, Journal of Materials Processing Technology 48/1-4 (1995) 727-737.

[13] L.A. Dobrzański, A. Zarychta, E. Hajduczek, M. Ligarski, Heat treatment of the Mo-V and W-V high-speed steels with addition of Ti, Silesian University of Technology Publishing House, Gliwice, 1997 (in Polish).

[14] O. Eso, Z. Fang, A. Griffo, Liquid phase sintering of functionally graded WC-Co composites, International Journal of Refractory Metals and Hard Materials 23 (2005) 233-241.

[15] L.A. Dobrzański, A. Kloc-Ptaszna, G. Matula, J.M. Torralba, Structure of the gradient carbide steels of HS6-5-2 high-speed steel matrix, Archives of Materials Science and Engineering 28/10 (2007) 589-592.